

Global Optimization of Two-input Systems using Multi-unit Adaptation

F. Esmailzadeh Azar, M. Perrier, B. Srinivasan

*Department of Chemical Engineering,¹
École Polytechnique Montréal,
Montréal, Canada, H3C 3A7*

Abstract: Model-free unconstrained real-time optimization can be realized by controlling the gradient to zero. In this paper, the multiunit optimization framework is used where the gradient is estimated using finite difference between two identical units operating with an offset. It has been recently shown that the global optimization is achieved by reducing this offset to zero for scalar nonlinear maps. In this paper, this scheme is extended to the case of two-input systems, by repeating mono-variable global optimization on the circumference of a circle of reducing radius. The theoretical concepts are illustrated on the global optimization of two examples.

1. INTRODUCTION

The main purpose of optimization is to improve the profit or reduce the operating cost, which is typically expressed as a nonlinear function of different decision variables. Finding the global optimum of an industrial process, has always been attractive in many engineering applications. Most of these problems are intrinsically multivariable.

For global optimization, many model-based deterministic (such as tight convex α BB underestimators for C^2 -continuous functions) or probabilistic approaches (such as random search and clustering) have been significantly developed during the last decades (Floudas et al., 2008). The deterministic methods exploit certain properties of the nonlinear function, while stochastic methods do not always guarantee convergence. These methods differ in terms of computational complexity, cost and accuracy.

On the other hand, in model-free real-time optimization methods, so-called extremum-seeking controllers, the unconstrained optimization problem is cast as a problem of controlling the gradient of the objective function to zero. For estimating the gradient, many techniques have been used: perturbations (Leblanc, 1922; Kritic, 2000), model-based (Guay et al., 2004) and multi-unit optimization (Srinivasan, 2007). These strategies lead to the closest local optimum depending on where the optimization starts. The framework used in this paper is the multi-unit optimization, that computes the gradient via finite difference between the outputs of multiple units with inputs that differ by a constant, pre-fixed offset (Srinivasan, 2007; Woodward et al., 2009). On the other hand, a global extremum seeking strategy based on perturbations (Tan et al., 2005, 2006a, b) was proposed,

where the amplitude of perturbation was reduced to zero. However, it has been shown that such a technique works for a restricted class of mono-variable nonlinear functions. As another alternative, it was recently shown in Azar et al. (2009a) that in the multi-unit optimization of a mono-variable system when the offset is reduced to zero, the scheme reaches the global optimum for all continuous nonlinear functions. Since the algorithm converges to a very small vicinity of the global optimum, it is so-called semi-global optimization. This technique was also extended to include inequality constraints (Azar et al., 2009b).

Local extremum-seeking techniques have been extended to the multi-variable setup; early multivariable extremum seeking schemes by Rotea (2000) and Walsh (2000) followed by a systematic design procedure provided by Ariyur et al. (2003). Teel and Popović (2001) studied sufficient conditions for the asymptotic stability of the smooth and non-smooth multivariable extremum seeking controllers that utilize some nonlinear programming algorithms.

In this paper, an extremum seeking strategy that converges to the global optimum of the static nonlinear continuous systems with two variables is proposed. This result is the extension of global optimization of mono-variable systems. The core idea is to iteratively perform mono-variable global optimization on the circumference of a circle of reducing radius. The radius of the circle is asymptotically reduced to zero. Also, relaxations of the algorithm are presented to make it numerically efficient.

The outline of the paper is as follows. Section 2 briefly reviews the local and global extremum seeking control using multi-unit optimization. Section 3 gives the extension of new algorithm with a discussion on the convergence result.

farhad.esmailzadeh-azar@polymtl.ca
michel.perrier@polymtl.ca
bala.srinivasan@polymtl.ca

Finally, the mentioned methodology is numerically simulated through some illustrative examples in section 4.

2. GLOBAL MONO-VARIABLE EXTREMUM-SEEKING CONTROL USING MULTI-UNITS

The multi-unit optimization method is a real-time extremum seeking technique that estimates the gradient by the finite difference of the outputs of two identical units where the inputs differ by an offset Δ (Srinivasan, 2007). An integral controller then forces the gradient to zero. The basic schematic of this technique (where Δ is fixed) converges to a local optimum of the objective function. It has been recently shown that global optimization of the nonlinear continuous static scalar maps can be achieved if Δ is monotonically reduced to zero (Azar et al., 2009a). This algorithm converges to an arbitrarily small vicinity of the global optimum of the static nonlinear continuous scalar maps (so-called semi-global optimization). The schematic is presented in Figure 1.

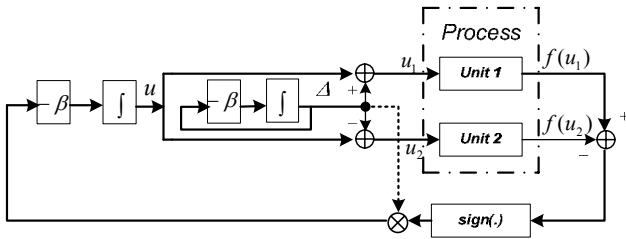


Figure 1: Global extremum seeking with multi units

The update equations and adaptation laws for global optimization (minimization) are given by,

$$u_1 = u + \Delta, \quad u_2 = u - \Delta \quad (1)$$

$$\dot{u} = -\beta\Delta \cdot \text{sign}(f(u + \Delta) - f(u - \Delta)), \quad u(0) = u_0 \quad (2)$$

$$\dot{\Delta} = -\beta\Delta, \quad \Delta(0) = \Delta_0 > 0 \quad (3)$$

where $\beta > 0$ is a parameter that determines the rate at which Δ is reduced to zero. It is important to note that only the unit with a lower objective function moves, while the one with the higher objective function stays at its current value.

It has been shown that this algorithm would reach to the global maximum provided the initial interval is large enough to include the global maximum. The proof of the result is based on the fact that the unique global maximum always lies within the interval $[u_1(t), u_2(t)]$ (Azar et al 2009a).

Also, the algorithm has been extended to the constrained global optimization of mono-variable systems where a switching adaptation law was used to handle the constraints (Azar et al., 2009b).

3. GLOBAL OPTIMIZATION OF TWO-INPUT SYSTEMS USING MULTI-UNITS

3.1 Construction of the algorithm

The main question that is addressed in this paper is how the global optimum of a two-dimensional map can be found in the multi-unit optimization framework.

Consider the problem of minimizing, $y = f(u_1, u_2)$, where $f: R^2 \rightarrow R$, is a non-convex continuous, nonlinear function. The problem may have multiple local optima, (u_{1k}^*, u_{2k}^*) , $k = 1, 2, \dots, n$, but a unique global minimum, (u_1^{**}, u_2^{**}) . In the rest of the paper, it is assumed that the global minimum is unique.

The proposed algorithm uses the spirit of the unconstrained scalar global optimization one. Here, we also need two identical units referred to as “a” and “b”. Let $(u_{1a}$ and $u_{2a})$ represent the first and second inputs of unit “a” and $(u_{1b}$ and $u_{2b})$ represent the inputs of unit “b”. The core idea of this algorithm is to perform global optimization on the circumference of a circle of reducing radius.

It is assumed that the feasible global optimum lies within the initial circle. The radius of this circle is reduced to zero in a predefined fashion. If the centre of the circle is so adapted as to keep the best optimum at the circumference, the algorithm converges to the global optimum of the nonlinear map when the radius goes to zero. In order to mathematically formulate the above mentioned methodology three iterative layers for the new optimization algorithm are considered:

Layer 1: Global optimization along the circumference of a circle

Consider a circle centred at the input values (u_1, u_2) and a radius of Δ (figure 2). The multi-unit optimization along the circumference of the circle of reducing radius is repeated iteratively. Let θ_a and θ_b be the angles of the two units.

Then the input values of the two units are given by:

$$\begin{cases} u_{1a} = u_1 + \Delta \cos(\theta_a) \\ u_{2a} = u_2 + \Delta \sin(\theta_a) \end{cases} \quad (4)$$

$$\begin{cases} u_{1b} = u_1 + \Delta \cos(\theta_b) \\ u_{2b} = u_2 + \Delta \sin(\theta_b) \end{cases} \quad (5)$$

The adaptation laws (for minimization) along the circumference of the circle are given by:

$$\theta_a = \theta + \Delta_\theta, \quad \theta_b = \theta - \Delta_\theta \quad (6)$$

$$\dot{\theta} = -\beta_\theta \Delta_\theta \cdot \text{sign}(f_a - f_b), \quad \theta(iT_+) = \pi + \theta_{mi} \quad (7)$$

$$\dot{\Delta}_\theta = -\beta_\theta \Delta_\theta, \quad \Delta_\theta(iT_+) = \pi \quad (8)$$

where Δ_θ is the offset between two angles θ_a and θ_b and $\beta_\theta > 0$ is a parameter that determines the rate at which Δ_θ is reduced. This corresponds to mono-variable global optimization along the circle of radius Δ using the angle θ . As will be discussed in the next section, the initial conditions of the equations (7) and (8) would be reinitialized

periodically. The period of the iteration (T) is so chosen that Δ_θ reduces to prefixed value ϵ_θ , i.e.

$$T = \frac{\ln(2\pi) - \ln(\epsilon_\theta)}{\beta_\theta} \quad (9)$$

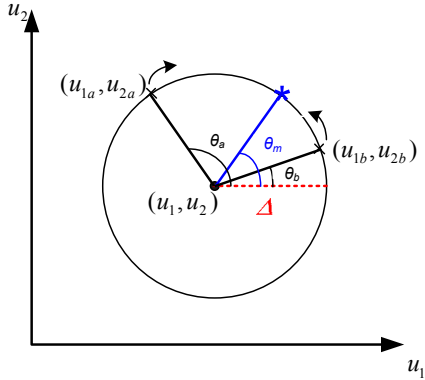


Figure 2: Global optimization along the circumference of a circle

Layer 2: Recursive global optimization

Let “ i ” denote the number of iteration ($i = 0, 1, 2, \dots$). At the beginning of each iteration, Δ_θ is initialized to π in order to cover the entire circle. The initial value of θ is so chosen to be the global optimum of the previous iteration.

At the beginning of first iteration (i.e. $i=0$), the initial value of θ_{m0} is arbitrarily set at zero. In the next iterations, θ_{mi} is computed from the values of θ_a and θ_b at the end of the previous iteration as follows

$$\theta_{mi} = \begin{cases} \theta_a(iT_-) & \text{if } f_a < f_b \\ \theta_b(iT_-) & \text{if } f_a \geq f_b \end{cases} \quad (10)$$

The optimization along the circumference is repeated every T time units. θ_{mi} corresponds to the converged value and would represent the global optimization along the circumference of the circle of iteration “ $i-1$ ” if $\epsilon_\theta = 0$.

Layer 3: Reducing the radius of the circle

It is assumed that the feasible global minimum lies within the initial circle (centred at the initial inputs $(u_1(0), u_2(0))$ with the radius of $\Delta(0)$). This radius is monotonically reduced to zero i.e.,

$$\dot{\Delta} = -\beta\Delta \quad \Delta(0) = \Delta_0 > 0 \quad (11)$$

$\beta > 0$ is a parameter that determines the rate at which Δ is reduced. The algorithm stops when Δ is reduced to a prefixed value ϵ . This means the time of integration of the algorithm is given by,

$$T_{tot} = \frac{\ln(\Delta_0) - \ln(\epsilon)}{\beta} \quad (12)$$

This way, the total number of iterations is fixed to T_{tot}/T . The coordinates which correspond to the global optimum of each iteration are as follows (Figure 4),

$$\begin{aligned} u_{1m} &= u_1 + \Delta \cos(\theta_{mi}) \\ u_{2m} &= u_2 + \Delta \sin(\theta_{mi}) \end{aligned} \quad (13)$$

where θ_{mi} corresponds to the global optimum of the previous iteration. The adaptation laws of the centre of the circle are so chosen to keep the global optimum found. In other words, the circle with the radius Δ and centre (u_1, u_2) is contracted in such a manner as to keep (u_{1m}, u_{2m}) at the same point i.e. $(\dot{u}_{1m}, \dot{u}_{2m}) = (0, 0)$. So, the adaptation laws are given by,

$$\begin{aligned} \dot{u}_1 &= -\dot{\Delta} \cos(\theta_{mi}) & u_1(0) &= u_{10} \\ \dot{u}_2 &= -\dot{\Delta} \sin(\theta_{mi}) & u_2(0) &= u_{20} \end{aligned} \quad (14)$$

This contraction is depicted in Figure 3. The centre of the circle is expected to converge to the global optimum of the non-linear map when Δ reaches to zero.

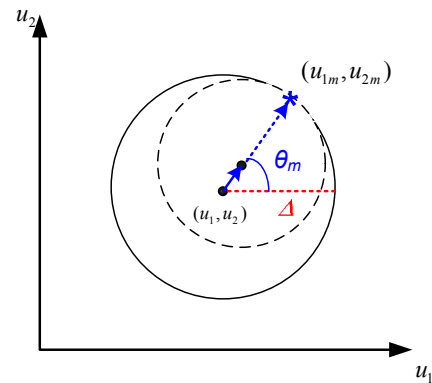


Figure 3: Contraction of the circle toward the global opt.

The structure of the above mentioned algorithm is presented in the following flowchart.

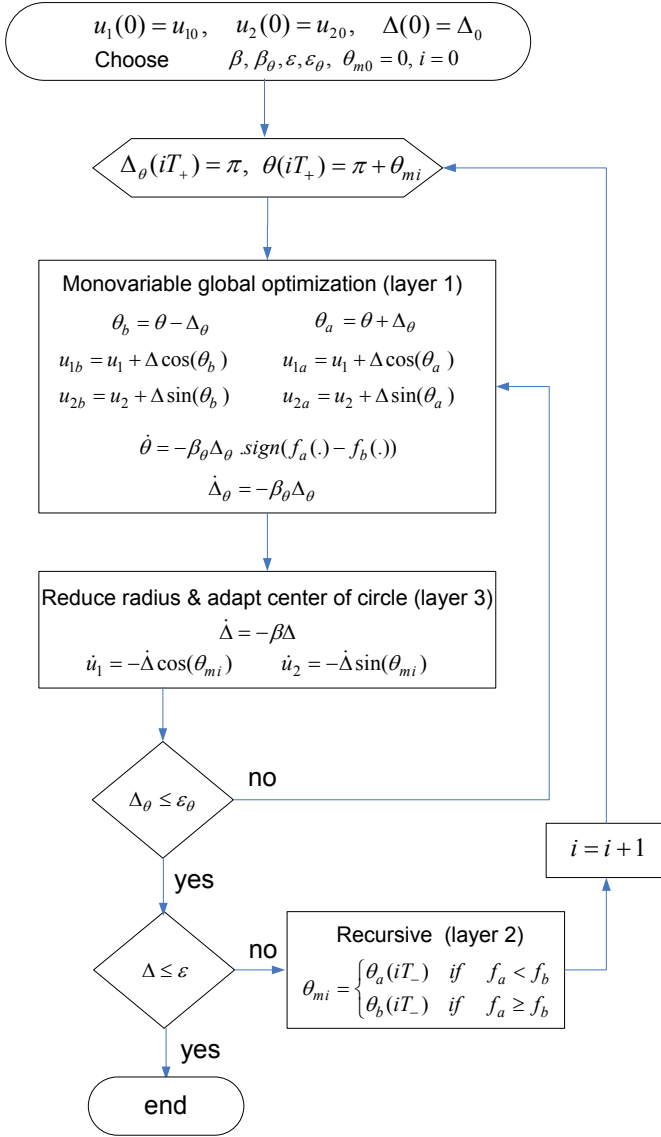


Figure 4: Flow chart of the global optimization of two input systems using multi-units

3.2 Convergence to the global optimum

For the general case, i.e. non-zero values of ϵ and ϵ_θ , it can not be guaranteed that the above scheme is indeed global. However, in the limiting case, it can be shown that this algorithm is capable of avoiding the local optima and converging to the global one.

Theorem 1: Consider the multi-unit optimization scheme with the adaptation laws (7), (8) and (11), (14), with $\epsilon=0$ and $\epsilon_\theta=0$. If (a) $f(\cdot)$ has a unique global minimum, (b) $\beta \ll \beta_\theta$ and (c) $(u_1^{**} - u_{10})^2 + (u_2^{**} - u_{20})^2 \leq \Delta_0^2$, then $u_1(\infty) = u_1^{**}$ and $u_2(\infty) = u_2^{**}$.

Proof: The proof of this result is based on the fact that there are two different time scales in the algorithm. The fast time scale is that of θ and Δ_θ , while the slow one consists of Δ , u_1 and u_2 . Initially it will be shown that the fast time scale keeps θ_{mi} at the global optimum along the circumference of the circle. Secondly, assuming this fact, it will be shown that the

shrinking of the circle leads to the global optimum of the problem. In fact, for θ_{mi} to always correspond to the global optimum, it is very important to have a good time scale separation between the two dynamics and the assumption $\beta \ll \beta_\theta$ is made towards this end.

To prove that θ_{mi} is in fact the global optimum along the circle, the proof follows the lines of (Azar et al., 2009a). At each iteration ($i = 1, 2, 3, \dots$) the mono-variable global optimization along the circumference would lead to, $|\theta(t) - \theta_i^{**}| \leq \Delta_\theta(t)$, $\forall t \in [iT_+, (i+1)T_+]$, where θ_i^{**} is the angle corresponding to the global optimum along the circle at iteration "i". So, when $\Delta_\theta \rightarrow 0$, then $|\theta(t) - \theta_i^{**}| = 0$, $\theta_a(iT_+) = \theta_b(iT_+) = \theta_i^{**}$ i.e. at the end of the iteration "i", $\theta_{mi} = \theta_i^{**}$.

Now, in a slower time scale, note that θ_{mi} is the global optimum along the circumference of the shrinking circle at any time. It will be shown by contradiction that $(u_1^{**} - u_1(t))^2 + (u_2^{**} - u_2(t))^2 \leq \Delta^2(t)$, $\forall t$. Suppose that at time instant t , $(u_1^{**} - u_1(t))^2 + (u_2^{**} - u_2(t))^2 > \Delta^2(t)$. From the hypothesis, $(u_1^{**} - u_{10})^2 + (u_2^{**} - u_{20})^2 \leq \Delta_0^2$, there exists a time instant $t = \tau$, such that $(u_1^{**} - u_1(\tau))^2 + (u_2^{**} - u_2(\tau))^2 = \Delta^2(\tau)$. This means that the global optimum of the map (u_1^{**}, u_2^{**}) is on the circle with centre $(u_1(\tau), u_2(\tau))$ and radius $\Delta(\tau)$. So, the angle search θ_{mi} would indeed latch on to this point (since the global optimum of the map is indeed the global optimum along the circumference of the circle). Also, in the next iteration $\theta_b(iT_+) = \theta_{mi}$, $u_{1b} = u_1^{**}$, $u_{2b} = u_2^{**}$ and,

$$\dot{\theta}_b = \dot{\theta} - \dot{\Delta}_\theta = -\beta_1 \Delta_\theta \cdot \text{sign}(f_a - f_b) + \beta_1 \Delta_\theta = 0 \quad (15)$$

Note that within the iteration, $\dot{\theta}_b = 0$, since $f_b < f_a$ is guaranteed by the uniqueness of the global minimum. Also, at the end of the iteration, θ_b will be retained as θ_{mi} since it has a better function value. Thus, once $(u_1^{**} - u_1(\tau))^2 + (u_2^{**} - u_2(\tau))^2 = \Delta^2(\tau)$, from there on for all $t > \tau$, $u_{1b} = u_1^{**}$ and $u_{2b} = u_2^{**}$.

Since $(u_{1b}, u_{2b}) = (u_1^{**}, u_2^{**})$ is on the circumference of the circle of radius $\Delta(\tau)$, it can be seen that $(u_1^{**} - u_1(t))^2 + (u_2^{**} - u_2(t))^2 = \Delta^2(t)$ for all $t > \tau$, which is a contradiction to the assumption $(u_1^{**} - u_1(t))^2 + (u_2^{**} - u_2(t))^2 > \Delta^2(t)$. So, it is deduced that $(u_1^{**} - u_1(t))^2 + (u_2^{**} - u_2(t))^2 \leq \Delta^2(t)$, $\forall t$.

Also, note that Δ is reduced to 0 monotonically, i.e. $\Delta(t) = \Delta_0 e^{-\beta t}$. In other words, when $\Delta \rightarrow 0$, $(u_1^{**} - u_1(\infty))^2 + (u_2^{**} - u_2(\infty))^2 = \Delta^2(\infty) = 0$, then $u_1(\infty) = u_1^{**}$ and $u_2(\infty) = u_2^{**}$.

Remark 1: Similar to what is stated in (Azar et al., 2009a), the sign function in the adaptation law (7) corresponds to a very high gain and induces a non-Lipschitz nature in the system. This might cause stiffness in integration. A simple solution is to replace the sign function by the hyperbolic tangent as shown below.

$$\dot{\theta} = -\beta_\theta \Delta_\theta \tanh(\eta(f_a - f_b)) \quad (16)$$

where η is a tuning parameter. The lower the value of η , the faster will be the integration. However, a low value of η might lead to a situation where the global optimum is missed and the algorithm converges to a local minimum. Thus, the value of η should be chosen as compromise between accuracy and integration time.

Remark 2: The basic condition for this algorithm to converge to the global optimum is $(u_1^{**} - u_{10})^2 + (u_2^{**} - u_{20})^2 \leq \Delta_0^2$. Since

the location of u^{**} is not known a priori, the above condition will be satisfied by choosing a large enough the initial value for Δ_0 . The downside of such a choice is that the algorithm requires more time to get to the optimum.

4. ILLUSTRATIVE EXAMPLES

Example 1: Consider the following nonlinear static map (Ackley's function shown in Figure 5) with a unique global minimum at $(u_1^{**}, u_2^{**}) = (0,0)$ and several other local optima (Molga et al., 2005).

$$f(u_1, u_2) = -20 \exp \left(-0.2 \sqrt{\frac{\sum_{i=1}^2 u_i^2}{2}} \right) - \exp \left(\sqrt{\frac{\sum_{i=1}^2 \cos(2\pi u_i)}{2}} \right) + 20 + \exp(1) \quad (17)$$

The important aspect of this example is the presence of equal valued and symmetric local optima on its nonlinear map.

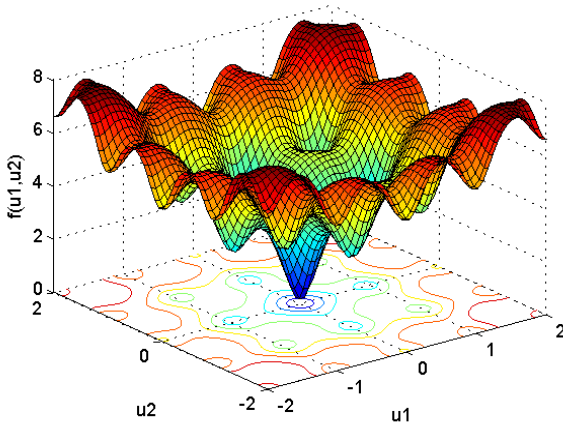


Figure 5: Static nonlinear map for Example 1

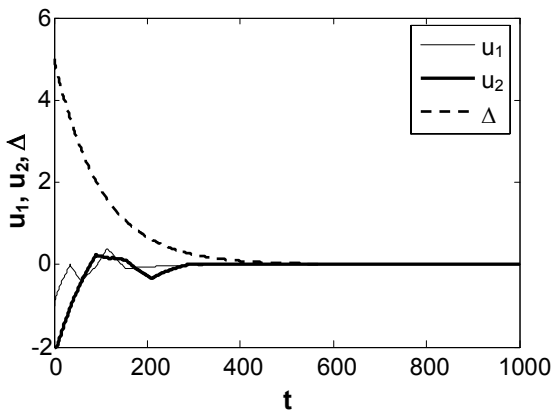


Figure 6: Evolution of the inputs and Δ for Example 1

The global optimization algorithm using two identical units is applied to optimize this nonlinear system. The initial inputs $u_{10} = -1$, $u_{20} = -2$, and $\Delta_0 = 5$ were considered such that the global minimum among the several other local ones lie in the circle composed by the centre of (u_{10}, u_{20}) and the radius of Δ_0 . The parameters used were $\beta = 0.01$, $\beta_\theta = 1$, and $\varepsilon = \varepsilon_\theta = 0.001$.

The time evolution of the inputs and Δ are shown in Figure 6. Using the adaptation as in (7) instead of (16) leads to a longer execution time of 12.18 sec., 120 iterations and 8200 number of function evaluations in contrast to 9.6 sec., 120 iterations and 6244 number of function evaluations in the later case with $\eta = 1$. Increase in execution time can be attributed to the increase in stiffness (Azar et al, 2009a).

Example 2: Consider the nonlinear Himmelblau's test function of order 4 (Pardalos et al., 2002) where the objective function on the global extremum $f(3,2)=0$ is very close the objective functions related to the other local optima,

$$\begin{aligned} f(-3.779310, -3.283186) &= 3.7979 \text{ e } -12, \\ f(-2.805118, 3.131312) &= 1.0989 \text{ e } -11, \\ f(3.584428, -1.848126) &= 8.8944 \text{ e } -12. \end{aligned}$$

The static map is depicted in Figure 7.

$$f(u_1, u_2) = (u_1^2 + u_2 - 11)^2 + (u_1 + u_2^2 - 7)^2 \quad (18)$$

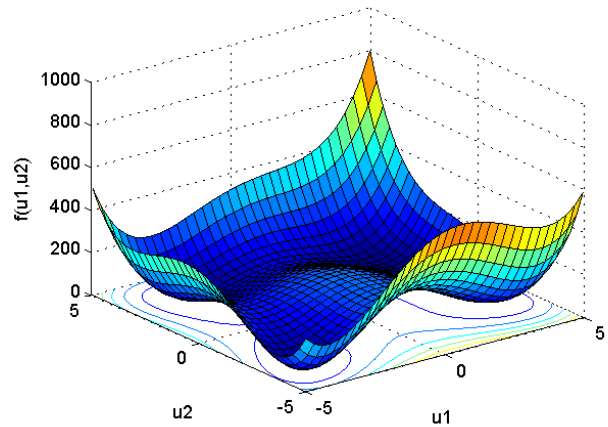


Figure 7: Static nonlinear map for example 2

The key condition to satisfy is the inequality $(u_1^{**} - u_{10})^2 + (u_2^{**} - u_{20})^2 \leq \Delta_0^2$ which is in fact verified by choosing $u_{10} = 3$, $u_{20} = -1$ and $\Delta_0 = 8$. The initial condition of u is chosen on purpose so as to be as closer to the local minimum which has the closest objective function to the global one. The other parameters were $\beta = 0.001$, $\beta_\theta = 0.01$, $\varepsilon = \varepsilon_\theta = 0.001$. Applying the global optimization algorithm using multiple units makes the system input to converge to the global minimum at $(u_1^{**}, u_2^{**}) = (3,2)$.

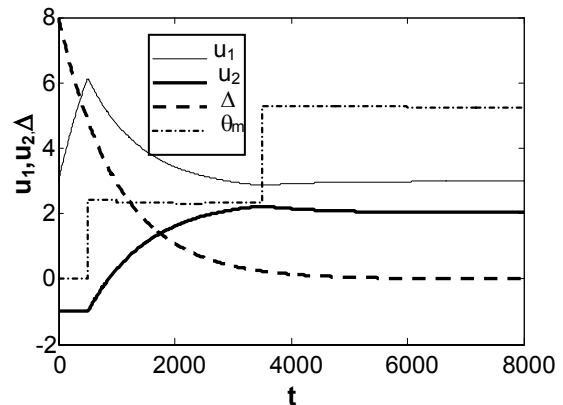


Figure 8: Evolution of the inputs, Δ and θ_m for Example 2

Fig (8) shows the time evolution of the angle θ_{mi} . It can be seen that the value of this angle evolves depending on the polar position of the global optimum found on the circumference of the shrinking circle. However, its value remains constant within the time interval of each iteration “i”.

It is equally interesting to see the evolution of θ_{mi} along the inputs and Δ . θ_{mi} remains unchanged as long as the global optimum found on the circumference of the shrinking circle remains unchanged. As soon as the system inputs pass through a better global optimum on the shrinking circle ($t=500$ sec), θ_{mi} latches on the angle corresponding to this point (2.4 rad.). Similarly at $t=3500$ sec., the system inputs find a better comparative global optimum on the circumference of the shrinking circle and this time θ_{mi} accords to the new value 5.27 rad.. Then, θ_{mi} remains unchanged until the complete contraction of the circle ($\Delta \rightarrow 0$). This means that the corresponding point to the last value of the angle θ_{mi} is the unique global optimum of the nonlinear map. It is clear that Fig (8) can be changed depending on the initial values of u_{10} , u_{20} , and Δ_0 (the initial circle) but the final converging results of the input values will be the same.

Choosing small initial value for offset $\Delta_0 = 2$ causes the algorithm to converge to the local minimum $(u_1, u_2) = (3.85, -1.85)$ instead of the global one. This is because the initial circle of $(u_1 - u_{10})^2 + (u_2 - u_{20})^2 = \Delta_0^2$ does not include the global minimum. In fact, the solution corresponds to the global minimum of this initial interval. An appropriate choice of η is crucial in converging to the global optimum. If a low value of $\eta = 1$ is chosen, the algorithm is mislead and converges to an optimum which is not global $(u_1, u_2) = (3.85, -1.85)$.

5. CONCLUSIONS

A model-free, unconstrained global optimization method using multi-units was proposed by controlling the centre of a shrinking circle on which the gradient is estimated using finite difference between two units operating with an offset.

For two-input systems, the technique was performed on the circumference of a circle of reducing radius. The offset parameter between the inputs of the two units was monotonically and iteratively reduced to zero where the radius of the circle was monotonically shrinking in parallel. With this, it was shown that it is possible to converge to the global optimum of any two dimensional nonlinear static objective function, provided the global optimum is present in the initial circle composed by the centre of the initial inputs and the initial value of the radius. Development of the proposed algorithm to systems with more than two degrees of freedom and to constrained optimization problems are the next steps considered in this research framework.

REFERENCES

Ariyur K.B. and M. Kristic (2003). *Real-time optimization by extremum-seeking control*, Published by John Wiley and Sons Inc. Hoboken, New Jersey, USA.

- Azar Esmailzadeh F., M. Perrier and B. Srinivasan, (2009a). Real-time global optimization using multiple units. *ICONS 2009, The 2nd IFAC International Conference on Intelligent Control Systems and Signal Processing*, Turkey.
- Azar Esmailzadeh F., M. Perrier and B. Srinivasan, (2009b). Real-time global optimization of constrained Non-linear systems using multiple unit optimization Scheme. *8th world congress of chemical engineering*, Montreal, Canada.
- Floudas C.A., C.E. Gounaris (2008). A review of recent advances in global optimization. *Journal of Global Optimization* DOI. 10.1007/s10898-008-9332-8.
- Guay M., D. Dochain and M. Perrier (2004). Adaptive extremum seeking control of continuous stirred tank bioreactors with unknown growth kinetics. *Automatica* 40, pp. 881-888.
- Kristic M., H. Wang (2000). Stability of extremum seeking feedback for general nonlinear dynamic systems. *Automatica* 36, pp. 595-601.
- Leblanc, M. (1922). Sur l'électrification des chemins de fer au moyen de courants alternatifs de fréquence élevée. *Revue générale de l'électricité* 12(8), 275-277
- Molga M. and Smutnicki C. (2005). Test functions for optimization needs, <http://www.zsd.ict.pwr.wroc.pl/files/docs/functions>
- Pardalos P., A. Migdalas and R. Burkard (2002). *Combinatorial and global optimization*, Published by World Scientific Publishing Co.Pte.Ltd. River Edge, USA.
- Rotea M. (2000). Analysis of multivariable extremum seeking algorithm. *Proc, American Control Conference*, Chicago, Illinois, June, pp. 433-437.
- Srinivasan B.(2007). Real-time optimization of dynamic systems using multiple units. *International Journal of Robust and Nonlinear Control*. DOI:10.1002/rnc.1165.
- Tan Y., D. Nešić and I.M.Y. Mareels (2005). On non-local stability properties of extremum seeking control. *Proc. 16th IFAC World Congress*, Prague, Czech Republic, pp. 2483-2489.
- Tan Y., D. Nešić and I.M.Y. Mareels and A. Astolfi (2006a). On global extremum seeking in the presence of local extrema. *Proceeding of the 45th IEEE Conference on Decision and Control*, San Diego, CA, USA.
- Tan Y., D. Nešić and I.M.Y. Mareels (2006b). On non-local stability properties of extremum seeking control. *Automatica*, 42, No.6, pp.889-903.
- Teel A.R. and D. Popović (2001). Solving smooth and nonsmooth multivariable extremum seeking problems by the methods of nonlinear programming. *Proc, American Control Conference*, Arlington, VA, June, Vol. 3, pp. 2394-2399.
- Walsh G. (2000). On the application of multi-parameter extremum seeking control. *Proc, American Control Conference*, Chicago, Illinois, June, pp. 411-415.
- Woodward L., Michel Perrier and B. Srinivasan (2009). Improved performance in the multi-unit optimization method with non-identical units. *Journal of Process Control*, Vol. 19, No. 2, pp.205-215.